

## Evidence for Changing of Cosmic Ray Composition between $10^{17}$ and $10^{18}$ eV from Multicomponent Measurements

T. Abu-Zayyad,<sup>1</sup> K. Belov,<sup>1</sup> D. J. Bird,<sup>5</sup> J. Boyer,<sup>4</sup> Z. Cao,<sup>1</sup> M. Catanese,<sup>3</sup> G. F. Chen,<sup>1</sup> R. W. Clay,<sup>5</sup> C. E. Covault,<sup>2</sup>  
J. W. Cronin,<sup>2</sup> H. Y. Dai,<sup>1</sup> B. R. Dawson,<sup>5</sup> J. W. Elbert,<sup>1</sup> B. E. Fick,<sup>2</sup> L. F. Fortson,<sup>2,\*</sup> J. W. Fowler,<sup>2</sup> K. G. Gibbs,<sup>2</sup>  
M. A. K. Glasmacher,<sup>7</sup> K. D. Green,<sup>2</sup> Y. Ho,<sup>10</sup> A. Huang,<sup>1</sup> C. C. Jui,<sup>1</sup> M. J. Kidd,<sup>6</sup> D. B. Kieda,<sup>1</sup> B. C. Knapp,<sup>4</sup>  
S. Ko,<sup>1</sup> C. G. Larsen,<sup>1</sup> W. Lee,<sup>10</sup> E. C. Loh,<sup>1</sup> E. J. Mannel,<sup>4</sup> J. Matthews,<sup>9</sup> J. N. Matthews,<sup>1</sup> B. J. Newport,<sup>2</sup> D. F. Nitz,<sup>8</sup>  
R. A. Ong,<sup>2</sup> K. M. Simpson,<sup>5</sup> J. D. Smith,<sup>1</sup> D. Sinclair,<sup>6</sup> P. Sokolsky,<sup>1</sup> P. Sommers,<sup>1</sup> C. Song,<sup>10</sup> J. K. K. Tang,<sup>1</sup>  
S. B. Thomas,<sup>1</sup> J. C. van der Velde,<sup>7</sup> L. R. Wiencke,<sup>1</sup> C. R. Wilkinson,<sup>5</sup> S. Yoshida,<sup>1</sup> and X. Z. Zhang<sup>10</sup>

<sup>1</sup>*High Energy Astrophysics Institute, University of Utah, Salt Lake City, Utah 84112*

<sup>2</sup>*Enrico Fermi Institute, University of Chicago, Chicago, Illinois 60637*

<sup>3</sup>*Smithsonian Astrophysics Observatory, Cambridge, Massachusetts 02138*

<sup>4</sup>*Nevis Laboratory, Columbia University, Irvington, New York 10533*

<sup>5</sup>*University of Adelaide, Adelaide S.A. 5005 Australia*

<sup>6</sup>*University of Illinois at Champaign-Urbana, Urbana, Illinois 61801*

<sup>7</sup>*University of Michigan, Ann Arbor, Michigan 48109*

<sup>8</sup>*Department of Physics, Michigan Technical University, Houghton, Michigan 49931*

<sup>9</sup>*Department of Physics and Astronomy, Louisiana State University, Baton Rouge, Louisiana 70803  
and Department of Physics, Southern University, Baton Rouge, Louisiana 70801*

<sup>10</sup>*Department of Physics, Columbia University, New York, New York 10027*

(Received 10 November 1999; revised manuscript received 4 February 2000)

The average mass composition of cosmic rays with primary energies between  $10^{17}$  and  $10^{18}$  eV has been studied using a hybrid detector consisting of the High Resolution Fly's Eye (HiRes) prototype and the MIA muon array. Measurements have been made of the change in the depth of shower maximum and the muon density as a function of energy. The results show that the composition is changing from a heavy to lighter mix as the energy increases.

PACS numbers: 96.40.De, 95.55.Vj, 96.40.Pq, 98.70.Sa

The source of cosmic rays with particle energies above  $10^{14}$  eV is still unknown. Models of origin, acceleration, and propagation must be evaluated in light of the observed energy spectrum and chemical composition of the cosmic rays. Several experiments have attempted to determine the mean cosmic ray composition through the "knee" region,  $10^{15}$ – $10^{16}$  eV, of the spectrum [1]. While the results are not in complete agreement, there is some consensus for a composition becoming heavier at energies above the knee, a result consistent with charge-dependent acceleration theories or rigidity-dependent escape models. In the region above the knee, the Fly's Eye experiment has reported a changing composition from a heavy mix around  $10^{17}$  eV to a proton dominated flux around  $10^{19}$  eV [2]. Muon data from the AGASA experiment show broad agreement with this trend if the data are interpreted using the same hadronic interaction model as in the Fly's Eye analysis [3,4].

Our experiment is unique in that two normally independent detection techniques are employed simultaneously in the measurement of various aspects of extensive air showers (EAS). We use a hybrid detector consisting of the prototype High Resolution Fly's Eye (HiRes) air fluorescence detector and the Michigan muon array (MIA). The detectors are located in the western desert of Utah at  $112^\circ$  W longitude and  $40^\circ$  N latitude. The HiRes detector is situated at a vertical atmospheric depth of  $860 \text{ g/cm}^2$  overlooking the MIA array which is 3.4 km away and 150 m lower.

The HiRes prototype [5] views the night sky over an elevation range from  $3^\circ$  to  $70^\circ$  with an array of 14 optical reflecting telescopes. They image the EAS as it progresses through the detection volume. Nitrogen fluorescence light (300–400 nm) is emitted at an atmospheric depth  $X$  in proportion to the number of charged particles in the EAS at that depth,  $S(X)$ . The measurements of the fluorescence efficiency and its temperature and pressure dependence on which this analysis is based are described in [6]. Part of this shower development profile (at least  $250 \text{ g/cm}^2$  long) can be determined by measuring the light flux arriving at the detector. Assuming  $S(X)$  to be the Gaisser-Hillas [7] shower development function and correcting for Cherenkov light contamination and atmospheric scattering effects one can measure both the primary particle energy  $E$  [via converting the total electromagnetic energy deposit which is proportional to the integral of  $S(X)$ ] and the depth at which the shower reaches maximum size,  $X_{\text{max}}$  [6].

MIA [8], consisting of over  $2500 \text{ m}^2$  of active area distributed in 16 patches of 64 scintillation counters, measures EAS muon arrival times with a precision of 4 ns. Such precise timing information is used to significantly reduce the systematic error in geometrical reconstruction. Improved precision in geometrical reconstruction translates into improved energy and  $X_{\text{max}}$  resolution. The average threshold energy for vertical muons is 850 MeV. MIA determines the muon density via the pattern of hit counters

observed in the shower [9]. An estimate of the muon density at 600 m from the core,  $\rho_\mu(600 \text{ m})$ , is then determined by a fit.

It is expected that changes in the mean mass of the cosmic ray flux as a function of  $E$  will be manifested as changes in the mean values of two measurable quantities  $X_{\text{max}}$  and  $\rho_\mu(600 \text{ m})$ . To indicate those changes, a rate of change of  $X_{\text{max}}$  with  $\log E$ , called the elongation rate,  $\alpha$ , has been introduced. Similarly for muons, we define a power law index for  $\overline{\rho_\mu}(600 \text{ m})$  as a function of  $E$ , called the “ $\mu$  content index,”  $\beta$ , in this study. Hence,

$$\alpha = \frac{d\overline{X}_{\text{max}}}{d \log E} \quad \text{and} \quad \beta = \frac{d \log \overline{\rho_\mu}(600 \text{ m})}{d \log E}. \quad (1)$$

Assuming that a shower initiated by a nucleus of mass number  $A$  and energy  $E$  is a superposition of  $A$  sub-showers each with energy  $E/A$ ,  $\overline{X}_{\text{max}} \propto \alpha_0 \log(E/A)$  and  $\overline{\rho_\mu}(600 \text{ m}) \propto A(E/A)^{\beta_0}$ , where  $\alpha_0$  and  $\beta_0$  are for a pure beam of primary nuclei of mass  $A$ . The values of  $\alpha_0$  and  $\beta_0$  are dependent on the hadronic interaction model, but we find them largely independent of  $A$  in our simulations described below. Therefore, any deviation of our observed elongation rate,  $\alpha$ , and  $\mu$  content index,  $\beta$ , from those for pure composition imply a changing composition, i.e.,

$$\frac{d \log \overline{X}_{\text{max}}}{d \log E} = -\frac{\alpha - \alpha_0}{\alpha_0} = \frac{\beta - \beta_0}{1 - \beta_0}. \quad (2)$$

Since the superposition model is not fully realistic, a more reliable comparison between the data and predictions is based on detailed simulation of shower development described below.

HiRes/MIA coincident data were collected on clear moonless nights between 23 August 1993 and 24 August 1996. The total coincident exposure time was 2878 h corresponding to a duty cycle of 10.2%. 4034 coincident events were observed. For events passing a set of coincidence assurance cuts the shower trajectory, including arrival direction and core location for each event, was obtained in an iterative procedure using the information from both HiRes and MIA [10]. The accuracy of the shower axis determination depends on the number of observed muons, the HiRes angular track length, and the core distances from MIA and HiRes. 2491 events are reconstructed via this procedure. Monte Carlo (MC) studies [11] show that the median shower direction error is  $0.85^\circ$  with a median core location error of 45 m. The energy  $X_{\text{max}}$  and  $\rho_\mu(600 \text{ m})$  are determined using this shower geometry as described above.

To ensure data quality and maintain good resolution we required that for each event  $X_{\text{max}}$  be visible within a minimum observed slant depth interval of  $250 \text{ g/cm}^2$  and that the track subtends at least  $20^\circ$ . Additionally, the  $X_{\text{max}}$  uncertainty had to be less than  $50 \text{ g/cm}^2$ , the reduced  $\chi^2$  for the profile fit could not exceed 10, the MIA to core distance  $R_{\text{pMIA}}$  had to be less than 2000 m, and the minimum pixel viewing angle had to be greater than  $10^\circ$ . These cuts left a sample of 891 events. Analysis involving  $\rho_\mu(600 \text{ m})$  required that the following additional cuts be

imposed:  $300 < R_{\text{pMIA}} < 1000 \text{ m}$ , and the number of hit MIA counters  $N_{\text{hit}} \leq 700$ . 573 events remained. Monte Carlo studies [11] using these cuts show that, averaged over the range of energies studied, the energy resolution is between 10% and 16% (iron showers and proton shower, respectively) and the  $X_{\text{max}}$  resolution is  $44 \text{ g/cm}^2$  for both shower types. These resolution figures are slow functions of energy. For example, for iron showers the resolution in energy changes from 11% at  $10^{17} \text{ eV}$  to 6% at  $10^{18} \text{ eV}$ , and the  $X_{\text{max}}$  resolution changes from 48 to  $41 \text{ g/cm}^2$  over the same range. In comparison, the energy resolution of the original Fly’s Eye experiment is 33% (single site) and 24% (stereo) below  $2 \times 10^{18} \text{ eV}$  [12]; the  $X_{\text{max}}$  resolution is about  $50 \text{ g/cm}^2$  averaged over a broader energy range up to  $10^{19} \text{ eV}$  [2]. The MIA resolution in  $\rho_\mu(600 \text{ m})$  is 30% and is independent of energy. It is largely determined by the resolution in core location, which is about 40 m.

The energy dependence of  $\overline{X}_{\text{max}}$  and  $\overline{\rho_\mu}(600 \text{ m})$  are shown in Figs. 1 and 2. The bands represent the statistical and systematic uncertainties in the mean values at each energy. The measured elongation rate is  $93.0 \pm 8.5 \pm (10.5)$   $(\text{g/cm}^2)/\text{decade}$  over the observed energy range. The measured  $\mu$  content index is  $0.73 \pm 0.03 \pm (0.02)$   $\text{decade}^{-1}$ . Bracketed numbers provide the systematic error based on the following discussion.

The systematic errors in  $\rho_\mu(600 \text{ m})$  stem from the uncertainties in the absolute efficiencies of the MIA counters over time. The average efficiency is 80.7% with an rms of 4.7% over the 16 patches during the time the data were taken. This is the only significant systematic uncertainty associated with  $\rho_\mu(600 \text{ m})$ .

For  $X_{\text{max}}$ , we have considered systematic errors in the atmospheric transmission of light and in the production

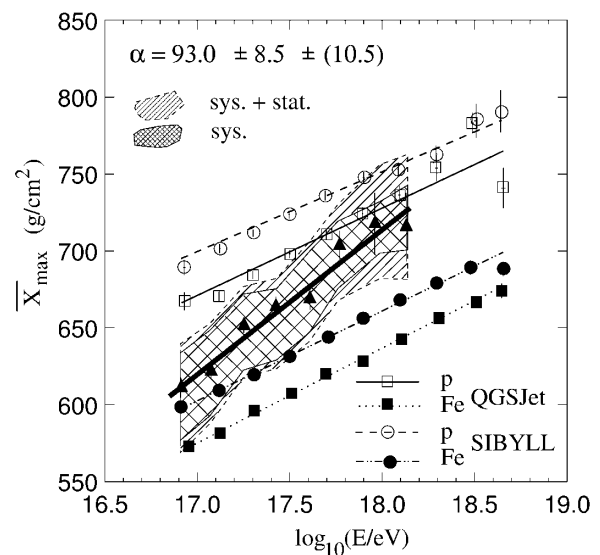


FIG. 1. Average  $X_{\text{max}}$  increasing with energy. Shaded areas and the thick line within the area represent HiRes data and the best fit of the data, respectively. The closed triangles represent the data set corresponding to the central values of the parameters in the reconstruction. The circles, squares, and lines refer to the simulation results. See text for details.

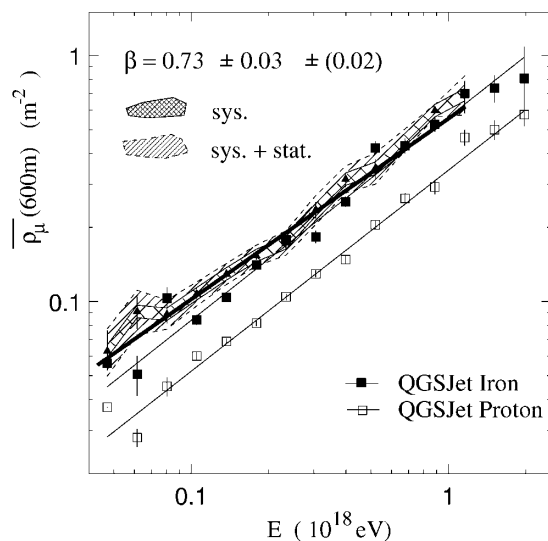


FIG. 2. Average muon density at 600 m from the shower core. Same as Fig. 1.

of Cerenkov light. These are related since atmospherically scattered Cerenkov light can masquerade as fluorescence light if not accounted for properly. For atmospheric scattering, there was uncertainty in the aerosol concentration and vertical distribution. The uncertainty, equivalent to 1 standard deviation about the mean, is expressed as a range of possible horizontal extinction lengths for aerosol scattering at 350 nm (taken as 11 to 17 km based on measurements using xenon flashers) [13] and a range of scale heights for the vertical distribution of aerosol density above the mixing layer (taken as 0.6 to 1.8 km). For Cerenkov light production, we have varied the angular scale for the Cerenkov emission angle over a 1 standard deviation equivalent. At ground level, we take the distribution as an exponential function of the angle from the shower axis, with a scale of  $4.0^\circ \pm 0.3^\circ$  [1]. Those uncertainties are shown by the shaded area in Fig. 1.

The systematic error in the energy is 25% and comes from fluorescence efficiency uncertainty [5], detector calibration uncertainty [14], and the atmospheric corrections [12]. The first two are intrinsically independent of the primary particle energy over this range. The fluorescence efficiency has been measured with an error of 10%. The percentage atmospheric corrections are also independent of energy because the sample of showers is restricted to core locations within 2 km of MIA center. Therefore there is no significant atmospheric path length difference between EAS and detector for different energies. An energy independent systematic fractional error in energy has no effect on the measured elongation rate and  $\mu$  content index. The magnitude of the systematic error in energy due to atmospheric attenuation can be estimated by varying the atmospheric parameters over the range described above. It is not greater than 10%. The detector calibration systematics is less than 5%.

Also shown in Figs. 1 and 2 are Monte Carlo simulation results. These full shower simulations have been per-

formed using the CORSIKA package [15], employing QGSJET [16] and SIBYLL [17] hadronic interaction models. We have generated 4000 showers covering the energy from  $3 \times 10^{16}$  to  $5 \times 10^{18}$  eV and at any zenith angle out to  $60^\circ$ . We then pass those showers through a realistic simulation of the detector with an energy spectrum starting at a minimum energy which is well below the HiRes/MIA threshold. 8000 proton and 4000 iron showers are generated with this detector simulation. With a thorough simulation of the fluorescence and Cerenkov light production, atmospheric molecular and aerosol scattering related attenuation, sky noise, geometric and electronic response of the detector and triggering, the generated events are passed through the same reconstruction and cuts as applied to the data. The simulated events show that the distributions of energy, impact parameter,  $R_p$ , and zenith angle are well predicted by the simulation [11]. The number of simulated iron showers is comparable with the experimental triggered event number, while we have doubled the proton events since they have more fluctuation in shower development. Both experimental and simulated event distributions show the same structure and tail behavior with similar statistics after reconstruction and cuts.

We find that a pure proton flux and the QGSJET model gives an elongation rate of  $\alpha_0 = 58.5 \pm 1.3$  ( $\text{g}/\text{cm}^2$ )/decade and a  $\mu$  content index of  $\beta_0 = 0.83 \pm 0.01$ /decade over the range from  $10^{17}$  to  $10^{18}$  eV. For a pure iron composition and the QGSJET model we find corresponding values of  $\alpha_0 = 60.9 \pm 1.1$  ( $\text{g}/\text{cm}^2$ )/decade and the same  $\beta_0 = 0.83 \pm 0.01$  ( $\text{g}/\text{cm}^2$ )/decade as for protons. Results from SIBYLL show similar elongation rates, but have the  $X_{\text{max}}$  approximately  $25 \text{ g}/\text{cm}^2$  deeper than QGSJET. SIBYLL also predicts significantly fewer muons at 600 m for both proton and iron showers. The effect of any triggering and reconstruction biases is very small for  $X_{\text{max}}$ , as can be seen in Fig. 1 by comparing these reconstructed data (dots) with the “input” (lines) directly from CORSIKA. The application of well chosen cuts has resulted in a bias-free measurement of the elongation rate. However, for muon density measurement, reconstruction effects change the index by 8%. We suspect that the presence of an asymmetry in core distance error can result in a small overestimate of the muon density. This effect may change with shower energy. We have looked into the possibility of a bias due to the influence of the maximum muon hit cut. However, low energy showers are detected with cores relatively close to MIA while higher energy showers have more distant cores. As a result, the number of muon counters hit is approximately independent of energy, resulting in minimal biasing.

We obtain an apparently larger elongation rate and a smaller  $\mu$  content index than those from the simulation based on a single chemical primary, either proton or iron. Both discrepancies, in the same direction, lend support to the hypothesis that the cosmic ray composition is changing towards a lighter mix of nuclei from  $10^{17}$  to  $10^{18}$  eV. HiRes and MIA reach the same conclusion by using different experimental techniques and measuring different

physics variables. Substituting the measured and simulated values of  $\alpha$  and  $\beta$  in (2) shows that the results from HiRes and MIA are consistent with an implied change in  $\Delta \ln A$  of about  $-1.28$  over one decade of energy.

It can be seen from Fig. 2 that at low energy the average measured muon density is larger than that predicted for pure iron showers. The predictions of  $\rho_\mu(600\text{ m})$  with SIBYLL (not shown) are even smaller. We have exhausted possible systematic differences between data and MC such as effects of cross talk, noise, punch through, and possible variation in the overburden. These effects were measured [8] and found to be negligible in their contribution to the observed difference. The value of  $\rho_\mu(600\text{ m}) = 0.24 \pm 0.02 \pm (0.02)\text{ m}^{-2}$  for this work is consistent with the AGASA experiment ( $\sim 0.25/\text{m}^2$  [3]) at  $3 \times 10^{17}$  eV. Although the atmospheric depth and threshold energy are different between the two experiments, a MC simulation based on CORSIKA using the QGSJET model shows that the resulting difference in  $\rho_\mu(600\text{ m})$  is about  $0.027\text{ m}^{-2}$ .

A shift of 40% in energy could eliminate the discrepancy between data and MC, but this is well beyond the systematic error of 25%. Such a shift would also produce large discrepancies in the distribution of geometrical variables between data and simulation. We conclude that the model is deficient in muon production. Evidence for this has also been found at lower EAS energies [18].

We conclude that the HiRes-MIA hybrid experiment confirms the Fly's Eye experiment result that the elongation rate is different from simulation with an unchanging composition, although the hadronic interaction models have been modernized and the detector resolution in energy and  $X_{\text{max}}$  is improved. Moreover, this confirmation is significant because of its unique combination of the simultaneous observation of shower longitudinal development and muon density on the ground. Within the error, the elongation rate observed in this experiment,  $93.0 \pm 8.5 \pm (10.5)\text{ (g/cm}^2\text{)}/\text{decade}$ , is consistent with  $78.9 \pm 3.0\text{ (g/cm}^2\text{)}/\text{decade}$  from Fly's Eye (quoted without systematic error) and that from Afanasiev *et al.* [19]. While the conclusion regarding the primary composition depends on the interaction model used, this study shows that the elongation rate is relatively stable with respect to choice of models. No modern interaction model has produced an  $\alpha_0$  much larger than  $60\text{ (g/cm}^2\text{)}/\text{decade}$ .

The Fly's Eye experiment [2] reports a change in the spectral index near  $5 \times 10^{18}$  eV in the stereo data. Such a break followed by a hardening of the spectrum has been interpreted as evidence for the emergence of an extragalactic component above a softer galactic component [2]. A change from a heavy to a light composition in this energy region also gives support to a changing origin for those cosmic rays. A number of new experiments, such as HiRes, the Pierre Auger Project, and the Telescope Array, could address this issue. However, the source of the lower energy

heavy composition remains a mystery. In that regard we note that there is a need to explore the energy region between  $10^{16}$  to  $10^{17}$  eV in order to connect our results with the measurements performed below  $10^{16}$  eV. A measurement of the composition in this region may be crucial for the understanding of the sources of cosmic rays above the "knee."

---

\*Joint appointment with The Adler Planetarium and Astronomy Museum, Astronomy Department, Chicago, IL 60605.

- [1] L. F. Fortson *et al.*, in *Proceedings of the 26th International Cosmic Ray Conference (ICRC), Salt Lake City, 1999* (University of Utah, Salt Lake City, 1999), Vol. 3, p. 125; K. H. Kampert *et al.*, *ibid.* Vol. 3, p. 159; F. Arqueros *et al.*, astro-ph/9908202.
- [2] D. J. Bird *et al.*, Phys. Rev. Lett. **71**, 3401 (1993).
- [3] N. Hayashida *et al.*, J. Phys. G **21**, 1101 (1995).
- [4] B. R. Dawson, R. Meyhandan, and K. M. Simpson, Astropart. Phys. **9**, 331 (1998).
- [5] T. Abu-Zayyad *et al.*, "The Prototype High Resolution Fly's Eye Cosmic Ray Detector," Nucl. Instrum. Methods Phys. Res., Sect. A (to be published).
- [6] R. M. Baltrusaitis *et al.*, Nucl. Instrum. Methods Phys. Res., Sect. A **240**, 410 (1985); R. M. Baltrusaitis *et al.*, in *Proceedings of the 19th International Cosmic Ray Conference, La Jolla, 1985* (NASA, Washington, DC, 1985), Vol. 7, p. 159; C. Song *et al.*, Astropart. Phys. (to be published), astro-ph/9910195.
- [7] T. Gaisser and A. M. Hillas, in *Proceedings of the 15th International Cosmic Ray Conference, Plovdiv, 1977* (Bulgarian Academy of Sciences, Plovdiv, 1977), Vol. 8, p. 353.
- [8] A. Borione *et al.*, Nucl. Instrum. Methods Phys. Res., Sect. A **346**, 329 (1994).
- [9] K. D. Green, in *High Energy Gamma Ray Astronomy*, edited by James Matthews, AIP Conf. Proc. No. 220 (AIP, New York, 1991), p. 184.
- [10] D. J. Bird *et al.*, "CASA-MIA-HIRES: A Hybrid Detector for Measuring Multiple Properties of  $10^{17}$  eV Extensive Airshowers" (to be published).
- [11] T. Abu-Zayyad *et al.*, in *Proceedings of the 26th ICRC* (Ref. [1]), Vol. 3, p. 260.
- [12] D. J. Bird *et al.*, Astrophys. J. **424**, 491 (1994).
- [13] T. Abu-Zayyad *et al.*, in *Proceedings of the 25th International Cosmic Ray Conference, Durban, 1997* (Potchefstroomse University, Potchefstroomse, 1997), Vol. 5, p. 345.
- [14] T. Abu-Zayyad *et al.*, in *Proceedings of the 26th ICRC* (Ref. [1]), Vol. 5, p. 429.
- [15] D. Heck *et al.*, University of Karlsruhe Report No. FZKA-6019, 1998.
- [16] N. N. Kalmykov, S. S. Ostapchenko, and A. I. Pavlov, Nucl. Phys. (Proc. Suppl.) **B52**, 17 (1997).
- [17] R. S. Fletcher *et al.*, Phys. Rev. D **50**, 5710 (1994).
- [18] M. A. K. Glasmacher *et al.*, Astropart. Phys. **12**, 1 (1999).
- [19] B. N. Afanasiev *et al.*, in *Proceedings of the Tokyo Workshop on Techniques for the Extremely High Energy Cosmic Rays, Tokyo, Japan, 1993*, edited by M. Nagano (Institute of Cosmic Ray Research, Tokyo, 1993), p. 35.